

A systematic investigation of the transfer of polyphosphate/inorganic silicate flame retardants from epoxy resins to layered glass fiber-reinforced composites and their post-furnace flexural properties

Sruthi Sunder¹ | Maria Jauregui Rozo² | Sneha Inasu¹ |
Bernhard Schartel²  | Holger Ruckdäschel¹ 

¹Department of Polymer Engineering,
University of Bayreuth, Bayreuth,
Germany

²Bundesanstalt für Materialforschung und
-prüfung (BAM), Berlin, Germany

Correspondence

Bernhard Schartel, Bundesanstalt für
Materialforschung und -prüfung (BAM),
Unter den Eichen 87, 12205 Berlin,
Germany.

Email: bernhard.schartel@bam.de

Holger Ruckdäschel, Department of
Polymer Engineering, University of
Bayreuth, Universitätsstraße 30, 95447
Bayreuth, Germany.

Email: holger.ruckdaeschel@uni-bayreuth.de

Funding information

Deutsche Forschungsgemeinschaft,
Grant/Award Numbers: AL 474/53-1,
SCHA730/26-1

Abstract

The systematic transfer of solvent-free, additive flame retardant (FR) formulations from epoxy resins to glass fiber-reinforced epoxy composites (GFRECs) through prepregs is difficult. Additionally, obtaining data on their post-fire mechanics is often challenging. Utilizing melamine polyphosphate (MPP), ammonium polyphosphate (APP), and silane-coated ammonium polyphosphate (SiAPP) FRs with low-melting inorganic silicates (InSi) in an 8:2 proportion and 10% loading by weight in a diglycidyl ether of bisphenol A (DGEBA) resin, a systematic investigation of the processing properties, room-temperature mechanics, and temperature-based mechanics of the systems was performed. The resin was cured with a dicyandiamide hardener (DICY) and a urone accelerator. The results revealed no substantial impact of these FRs at the current loading on the resin's glass transition temperature or processability. However, the fire residues from cone calorimetry tests of the composites containing FRs were found to be only 15-20% of the thickness of the resins, implying a suppression of intumescence upon transfer. At room temperature, the decrease in the flexural modulus for the composites containing FRs was negligible. Exposure of the composites in a furnace at 400°C as a preliminary study before ignition tests was shown to cause significant flexural moduli reductions after 2.5 min of exposure and complete delamination after 3 min making further testing unviable. This study emphasizes the need for future research on recovering modes of action upon transfer of FR formulations from resins to composites. Based on the challenges outlined in this investigation, sample adaptation methods for post-fire analysis will be developed in a future study.

Sruthi Sunder and Maria Jauregui Rozo contributed equally to this work.

This is an open access article under the terms of the [Creative Commons Attribution](https://creativecommons.org/licenses/by/4.0/) License, which permits use, distribution and reproduction in any medium, provided the original work is properly cited.

© 2024 The Authors. *Polymer Composites* published by Wiley Periodicals LLC on behalf of Society of Plastics Engineers.

Highlights

- Processibility of resins for prepreg production unaffected by polyphosphate/inorganic silicate flame retardants (FRs).
- FR formulations had a negligible effect on the mechanics of the composites.
- 15%–25% increase in the fracture toughness of the DGEBA-based resin matrix with FRs.
- Suppression of intumescent behavior in the composites verified quantitatively.
- Significant reduction in flexural moduli of the composites post-400°C exposure in a furnace.

KEYWORDS

DGEBA, glass fiber-reinforced composites, post-furnace testing, prepregs

1 | INTRODUCTION

Together, the transportation and construction industries accounted for about 43% of the total consumption of epoxy resins within Europe alone, amounting to a production volume of around 138,000 tonnes just in 2019.¹ The modification of epoxy resins (EP) systems and glass fiber-reinforced epoxy composites (GFRECs) for flame retardancy applications in these industries is critical, owing to the wide range of material characteristics of these resin systems, including highly desirable mechanical properties, easy processing, low shrinkage during resin curing, and good adhesion to glass fibers.² Additionally, due to their capacity to allow light weighting, GFRECs are in high demand to reduce the overall mass of trains, ships, or airplanes and thus increase fuel efficiency.^{3,4} This study is carried out on diglycidyl ether of bisphenol A (DGEBA), chosen as the matrix due to its potential universal applications ranging from electrical parts to the aerospace industry.⁵ However, DGEBA is highly flammable, thus requiring the use of additives to enhance its flame retardancy.⁶ Several studies in the literature exist for the processability of FRs in neat resins (NR), especially for solvent-based systems such as those containing reactive flame retardant moieties^{7–9} and non-reactive phosphorous compounds such as 9,10-dihydro-9-oxa-10-phosphaphenanthrene-10-oxide (DOPO).^{10–12} However, studies on the transfer of solvent-free, dispersed FR formulations from EP resins to glass fiber (GF)-reinforced epoxy composites (GFRECs) via prepregs are limited^{13–15} and require systematic investigation. This study thereby seeks to investigate the processing and thermomechanical properties of DGEBA resins with three non-halogen-based intumescent/low-melting glass FR solid filler combinations in an EP matrix. The transferability of these resins to GFRECs via prepregs is a vital focus of this study. Here, three intumescent: ammonium polyphosphate (APP), melamine polyphosphate (MPP),

and silane-coated APP (SiAPP), are combined with low melting glass, and compared for their processability in EP for transfer to GFRECs. Shear viscosity measurements are used to screen potential formulations for transfer to prepregs and to identify key processing parameters. Formulations containing 10% w/w MPP/APP/SiAPP and InSi in DGEBA are transferred to unidirectional (UD) bidirectional (BD) GFRECs with glass fiber densities of approximately 600 g/m² via prepregs. Studies on the post-fire mechanics of such composites are even more scarce due to difficulties in balancing fire exposure test parameters with matrix delamination and resin-burn off effects that make sample testing unviable. These investigations would aid in processing formulations for further investigations in comparing the pre-, in-fire, and post-fire mechanical properties and flame retardancy behavior of the flame-retardant NRs after transfer to the GFRECs. As an initial test, standard three-point bending samples are exposed to heat in a furnace oven to gauge the reduction in their flexural properties.

2 | BACKGROUND

Despite the disadvantages of using dispersed fillers, such as filtration effects when transferred to reinforcing fibers, they are advantageous due to their cost effectiveness and low processing requirements.¹⁶ Phosphate-based fillers such as APP or MPP are well-established FRs for use in various types of EPs.^{17–19} In 2022, Elejoste et al.²⁰ studied the transfer of various additive flame retardant formulations in a furan-based resin for transfer to basalt fiber reinforcements. They reported that APP was effective in producing an intense dehydration effect in both the resin and the composite. The pyrolytic degradation primarily results in water and ammonia elimination, the latter acting in the gas phase. Further, the formation of polyphosphoric acid at temperatures above 250°C, and consequent acid evaporation and dehydration results in intumescent behavior

and the formation of a carbonaceous char layer on the surface of the polymer. However, furan resins possess inherently good flame retardant and charring behavior in comparison to DGEBA resins, which limits the study's applicability only to inherently flame-retardant resins. Zhang et al.²¹ reported the enhancement of the interaction between APP and DGEBA using hydrophobic modification with cationic latex. In this study, APP is additionally compared with silane-coated APP for its improved processability in EP resins in addition to lower solubility in water or organic solvents.²² An earlier study by Döring et al.²³ showed that MPP enhances the capability of organophosphorus flame retardants to replace halogenated flame retardants due to the intumescent behavior of MPP, similar to APP with the melamine species instead being the source for the ammonia and char. Similar to the study by Elejoste et al.,²⁴ the resin system used by Döring et al. was epoxy novolac (DOW DEN 438), which also possesses some level of inherent flame retardancy due to its higher functionality. Ricciardi et al.²² compared the behavior of MPP, APP, and SiAPP in unsaturated polyester resins at loadings of 20% and 35% w/w. They found that it is possible to use APP without smoke suppressors to reduce smoke release parameters. APP performed better than MPP and SiAPP in lowering heat release parameters in the polyester resin. To improve the consolidation of the intumescent residue and to improve the fire residue stability, Wu et al.²⁵ investigated the effect of the addition of low-melting inorganic silicates (InSi) in a layered epoxy-clay composite system. They found that a loading level of 10% w/w is optimum for improving fire performance. However, due to its coarse nature, the commercial variant of low-melting glass (LMG) used in their study requires further refinement via ball milling and sieving, as described by Liu et al.,²⁶ before processing. Thus, inorganic low-melting glass frits with narrow particle size distributions are used in this paper for easier processing. In this same study, Wu et al. showed that a combination of LMG and APP in the ratio of 8:2 with a total loading of 10% w/w in an EP resin system was optimal in creating an effective fire barrier while lowering the total heat release (THR) of the system in cone calorimetry tests (CCTs). They also stressed the importance of the melting temperature of the glasses in creating such a barrier compared to the central temperature of a burning polymer.

Thus, although such studies and more^{23,27,28} identify synergistic and additive combinations of flame retardants (FRs) for non-intrinsically flame retardant EP resins, systematic investigations into their processability and data on transferability to prepregs are less available. Loading levels of these fillers can affect the rate of filtration or aggregation effects, especially in the small intra-tow gaps between 0/90° GF tows. These phenomenon can also affect processability and the overall properties of the

GFRECs, as reported by Pawellski-Hoell et al.¹⁵ They also showed that high loading levels of fillers (>40% w/w) can increase the viscosity and curing kinetics of the resin, creating a need to balance the processing parameters such as the film coating unit or heating unit speed and temperatures when transferring these resins to composites via prepregs. The inclusion of mineral fillers such as ATH in a polymer matrix can effectively reduce the risk of fire. However, due to high load requirements, this can cause processing limitations due to increasing viscosity and a significant reduction in mechanical performance. Thus, considering lower filler dispersion weights is a first step towards improving the processability of the resins for subsequent transfer to prepregs, which can be fulfilled by using compatible fillers such as APP or MPP. Moreover, despite some investigations available in the literature on phenolic-based epoxy systems,^{29–31} the post-fire flexural properties of DGEBA-GFRECs have not yet been reported extensively. These are due to difficulties in balancing test parameters with resin-burn-off and composite delamination, as well as a lack of testing norms for post-fire flexural testing of composites.

3 | EXPERIMENTAL SECTION

3.1 | Resins and composites preparation using prepregs

3.1.1 | Materials

Tables 1–3 summarize the details of the resin formulations, flame retardant fillers, and reinforcing fibers used in this study. The reference EP system (E100) was prepared using DGEBA:DICY:UR400 in the stoichiometric ratio of 100:6.5:1 based on Equation (I)³²:

$$\text{PHR} = \left[\frac{100 \times (\text{AHEW}_{\text{curing agent}})}{(\text{EEW}_{\text{epoxy resin}})} \right] \quad (\text{I})$$

PHR is the amount of the curing agent in parts per hundred in the resin, AHEW is the Amine Hydrogen Equivalent Weight of the curing agent and EEW is the epoxy equivalent weight of the DGEBA resin. FR EP formulations, as shown in Table 4, were prepared at 10% w/w in the resin, keeping the ratio of the intumescent to the InSi constant at 8:2. The curing agents and fillers were dispersed in the resin using a dual asymmetric centrifuge speed mixer by Hauschild Engineering (from Hamm, Germany) for 2 min at the rate of 3000 rpm for homogenizing the resin. The formulations were degassed at 15–20 mbar for a minimum of 10 min under vacuum to remove the built-up air introduced during mixing. The

TABLE 1 Summary of resin components and their chemical structures.

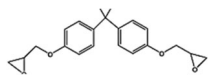
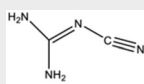
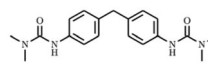
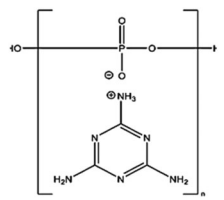
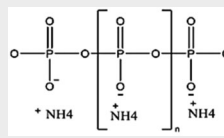
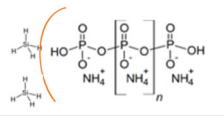
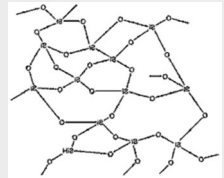
Material	Purpose/Commercial name/Supplier	Properties	Structure
Diglycidyl ether of bisphenol A (DGEBA)	EP resin matrix/DER 331/Olin Epoxy	EEW: 182–192 g/eq Viscosity (25°C): 11–14 Pa.s Density (25°C): 1.16 g/cm ³	
Dicyandiamide (DICY)	Hardener/DYHARD 100S/Alzchem	Melting point ~ 210°C d_{98} : <10 μm	
Urone (UR400)	Accelerator/DYHARD UR400/Alzchem	Melting point: 220°C d_{98} : <10 μm	

TABLE 2 Summary of flame-retardant additive components and their chemical structures.

Material	Purpose/Commercial name/Supplier	Properties	Structure
Melamine polyphosphate (MPP)	Intumescent flame retardant/FR CROS 513/ Budenheim	P ₂ O ₅ : 30%, N: 43%; pH: 6; T _D : 325°C; d_{50} = 8 μm	
Ammonium polyphosphate (APP)	Intumescent flame retardant/FR CROS 484/ Budenheim	P ₂ O ₅ : 72%, N: 14%; pH: 5.5; T _D : 300°C; d_{50} = 18 μm	
Silane-coated ammonium polyphosphate (SiAPP)	Coated APP to improve resin dispersion/FR CROS 486/Budenheim	P ₂ O ₅ : 72%, N: 14%; pH: 7; T _D : 250°C; d_{50} = 18 μm	
Inorganic silicate/glass frits (InSi)	Low melting glass to create a fire barrier and stabilize fire residue/Flamtard V100/William Blythe	d_{50} = 5 μm	

mixture was then poured into preheated molds of varying thicknesses depending on the tests to be carried out. These mixtures were then cured in a Memmert ULE 400 convection oven from Memmert GmbH, Germany. Here, an initial ramp up to 100°C for 2 h, followed by a second ramp up to 140°C for 2 h was used for curing. Afterwards, the molds were cooled overnight to obtain EP resin plates.

3.1.2 | Preparation of flame-retardant formulations for preregs and composites

Resin mixing

The resins were prepared in the proportions as detailed in Section 3.2 without using solvents. For ease of processing, the DGEBA resin was pre-heated to 50°C using a Memmert ULE 400 convection oven. The curing agents

and FRs were dispersed using a mechanical stirrer at 1000 rpm for 10 min and degassed at 15–20 mbar for a minimum of 10 min under vacuum to remove the built-up air introduced during mixing. The high shear forces help ensure proper wetting and homogenous dispersion of the fillers in the resin.

Prepreg processing

The preregs were manufactured at Neue Material Bayreuth GmbH, Germany, on a lab-scale prepreg line from EHA Composites Machinery, Germany. To avoid thinning of the resins, they were added to the coating unit at room temperature (25°C) via direct film-coating on a siliconized release paper and a line speed of 1.5 m/min. The resins impregnate the glass fabrics in the calendar unit at 50°C while covered using siliconized paper. The resin is coated to a width of 220 mm on the glass fabric which has an

overall width of 300 mm, rolled, vacuum sealed and stored at -18°C . The UD and BD fibers are fed in the 0° fiber orientation.

Laminate production in the autoclave

The UD GF prepregs with a width of 220×300 mm were layered and stacked by hand layup on a steel plate covered with smooth laminating foil. These were then vacuum bagged and cured in an autoclave setup under vacuum (<20 mbar) with no additional air pressure using a first curing ramp of 100°C for 2 h followed by a second ramp to 140°C for 2 h and finally, a cooldown ramp to room temperature for 4 h. The basis for choosing the curing profiles is described in the results from rheology and DSC data. The final laminate thicknesses for all the composite formulations were found to be on average, 2.5 ± 0.3 mm using five layers of GF and 4.4 ± 0.3 mm using nine layers of GF for the GFRECs.

3.2 | Characterization methods

3.2.1 | Processing, curing parameters, and additive particle size distribution

Rheology

The processibility of the flame-retardant combinations as additives for the DGEBA systems was measured using an

TABLE 3 Summary of glass fiber constructions used as reinforcements.

Material/Supplier	Configuration
Bidirectional layered glass fibers G600BD-1300/Saertex GmbH	0° E glass 1100 tex: 346 g/m^2
	90° E glass 600 tex: 283 g/m^2
	Backing yarn PES 110 dtex: 3 g/m^2
Unidirectional layered glass fibers UE640-1300/Saertex GmbH	0° E glass 1200 tex: 567 g/m^2
	$+45^{\circ}$ E glass 68 tex: 13 g/m^2
	90° E glass 68 tex: 13 g/m^2
	-45° E glass 68 tex: 13 g/m^2
	Backing yarn PES 76 dtex: 3 g/m^2

TABLE 4 Summary of flame-retardant resin formulations by weight.

Sample label	Material quantity in % w/w						
	Active FR %		DGEBA + DICY + UR400 (E)	InSi	MPP	APP	SiAPP
	P	N					
E100	0	0	100	0	0	0	0
E90InSi10	0	0	90	10	0	0	0
E90InSi2MPP8	1.4	3.2	90	2	8		
E90InSi2APP8	3.75	1.3	90	2		8	
E90InSi2SiAPP8	3.75	1.3	90	2			8

Note: The particle size distributions of the filler mixtures were measured via dynamic light scattering (DLS) (see Supplementary information).

Anton Paar Rheometer (MCR 301). The rheological properties of the uncured samples were then evaluated within the linear viscoelastic region using a parallel plate (PP25) with a gap between parallel plates of 1 mm in the range of $25\text{--}200^{\circ}\text{C}$ at a $3^{\circ}\text{C}/\text{min}$ temperature ramp. The complex viscosities of the resin formulations were tested to ensure that they lie between 10 and 50,000 mPa s for optimal prepreg processing in the plant line.³³ The initial minimum viscosity, as well as the gel points of the formulations, were analyzed.

Differential scanning calorimetry (DSC)

The curing onset, complete cure, as well as curing enthalpy were analyzed from the first heating cycle using dynamic DSC measurements. A Mettler Toledo DSC 1 (Columbus, Ohio, USA) was used for this purpose using a heating ramp rate of 10 K/min and a measurement range from 25 to 275°C . The nitrogen flow rate was set to 50 mL/min, and the sample mass used was 20 ± 2 mg. Two iterations of the test were performed per sample.

Dynamic light scattering (DLS)

To assess the particle size distributions of the combinations of FRs used in the E90InSi2MPP8, E90InSi2MPP8, and E90InSi2MPP8 resin formulations, the particle size distributions of the various combinations of the flame retardants used were analyzed using dynamic light scattering. This was done using a Mastersizer 2000 from Malvern Instruments by preparing an 8:2 mixture of MPP/APP/SiAPP + InSi homogenized by hand and dispersing in water. The d_{50} and d_{90} of the particles are then assessed within the system using the Stokes–Einstein Equation.

3.2.2 | Resin and prepreg quality analysis

Surface morphology using scanning electron microscopy (SEM)

The cured surfaces of the resins and the composite samples embedded in an DGEBA epoxy resin and hardener using embedding springs (EpoFix from Struers,

Denmark) for visualization were analyzed using a Zeiss Gemini 1530 Scanning Electron Microscope from Carl Zeiss AG. The sample surfaces were sputtered using platinum up to a thickness of 5 nm. An acceleration voltage of 3 kV was used.

Fiber volume content (FVC)

The final FVC of the prepregs was obtained in two ways. First, the prepregs were checked in-process by weighing a circular piece of fabric of diameter ~ 10 cm cut out from the impregnated GFs in the resin line, which was compared to the weight of the non-impregnated glass fiber. Second, the cured composite samples weighing 15–20 mg were heated at rates of 10 K/min in a thermogravimetric analysis (TGA) setup with an initial and final temperature of 25 and 800°C in synthetic air. Since the overall loading of the InSi was only at 2% w/w in the resin matrix, this aspect was not considered since the amount on transfer to composites would be negligible.

3.2.3 | Mechanical behavior

Fracture toughness (K_{IC} and G_{IC})

The mode I fracture toughness K_{IC} and G_{IC} were determined according to ISO 13586 on a Zwick testing apparatus with a load cell capacity of 20 kN. A minimum of eight specimens were tested per sample.

Dynamic mechanical analysis (DMA)

Dynamic mechanical analysis (DMA) under and above the glass transition temperature (T_g) was carried out on a Gabo Eplexor 500 N. The neat resin, and UD and BD composite samples were all measured in torsion mode. The specimens were cut to dimensions of 50 mm by 10 mm by 2 mm and were measured using a temperature range from 25 to 180°C under a temperature ramp of 3 K/min. The UD fibers were loaded in the 90° direction to the clamps. The glass transition temperature (T_g) was observed as the maxima of the loss factor ($\tan \delta$). Three specimens were tested per sample type.

Flexural behavior at room temperature and after furnace radiation exposure

For the analysis of the flexural behavior of the resins, six specimens with dimensions 80 × 10 × 4 mm were tested using a three-point bending apparatus. The machine was set up according to ISO 178 using a crosshead speed of 2 mm/min on a Zwick Roell Z020 originally from Zwick Roell GmbH & Co. KG (Ulm, Germany). The capacity of the load cell used was 20 kN. The composite samples were similarly analyzed using the DIN EN ISO 14125 standard with dimensions of 100 × 15 × 4 mm.

Separately prepared composites were then exposed to radiation in a furnace oven at 400°C for 1.5 and 2.5 min, and subsequently tested via three-point bending.

Interlaminar shear strength (ILSS)

The maximum shear strength τ was obtained by ILSS analysis according to DIN EN 2563 with the UD and BD composite specimens of 10 mm in width and 20 mm in length. The samples were tested on a Zwick Z050 apparatus at room temperature. A span:thickness ratio of 5:1 was maintained in the apparatus, and the loading cylinder was maintained at a constant crosshead speed of 1 mm/min.

3.2.4 | Fire behavior and residue analysis

Samples with a width and length of 100 mm × 100 mm and thickness of 4.0 ± 0.3 mm for the FR resins, UD, and BD GFRECs were exposed to a heat flux of 50 kW/m² and a distance from the sample to the heat source was set to 35 mm in a Dual Cone Calorimeter (Fire Testing Technology Ltd., East Grinstead, UK). This distance was set in order to allow room for growth of the intumescent samples during burning, without changing the effective heat flux at the surface of the sample.³⁴ The thickness of the fire residue in the samples was measured, and the fire residues from the burnt samples were checked for delamination in the case of the GFRECs.

4 | RESULTS AND DISCUSSION

4.1 | Processability of the flame-retardant resin formulations

4.1.1 | Differential scanning calorimetry (DSC)

The first heating cycles performed via DSC for the various resin formulations in comparison to the reference systems are depicted in Figure 1, and these are used to compare the onset of curing, peak curing, and curing enthalpy of the systems, the data for which is shown in Table 5. Detailed investigations using varying heating rates to determine the resin's curing behavior have already been conducted elsewhere.^{35,36} The onset of curing temperature shows similar behavior to the gel point of the systems containing FRs compared to the reference system. Their values lie between the reference systems E100 (onset: $145 \pm 0.4^\circ\text{C}$) and E90InSi10 (onset: $149 \pm 1^\circ\text{C}$, peak: $153 \pm 0.7^\circ\text{C}$). The replacement of the InSi here also brings the onset of curing closer to the reference value of E100. The negligible change in the onset of curing is possibly

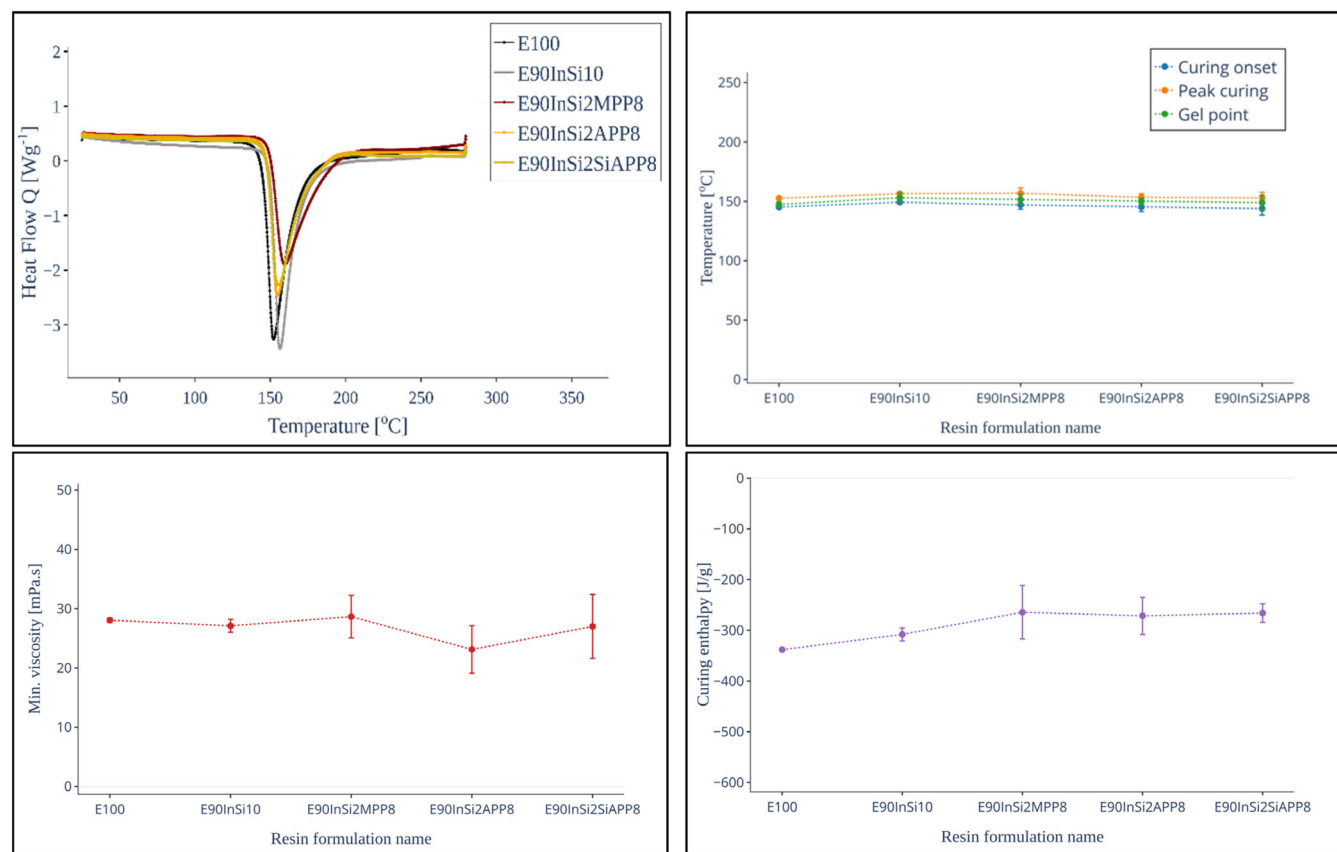


FIGURE 1 DSC curves of the first heating cycle of the various resin formulations (top left) and comparison of various curing properties of the resin formulations gel point, curing onset, and peak curing temperatures (top right) minimum viscosity (bottom left), curing enthalpy (bottom right).

related to an increase in nucleation sites or increased surface area to initiate the epoxy curing reaction for all the systems with FRs. The peak of curing is also negligibly higher than the reference E100 at $153 \pm 0.7^\circ\text{C}$. This is likely because the fillers themselves do not actively participate in the chemical curing process and act as inert additives. The curing enthalpy of all the systems containing FRs are higher than the references E100 and E90InSi10 at -341 ± 4 and -317 ± 13 J/g, respectively, indicating decreasing exothermicity of the reactions. The dispersed fillers act as small heat sinks, resulting in a higher heat capacity absorption during the curing process.

Thus, a curing temperature of 100°C for 2 h followed by post-curing at 140°C for 2 h was chosen, which verifies the manufacturer's recommendation for curing DGEBA + DICY + urone resin-hardener-accelerator systems prepared in the stoichiometric ratio of 100:6.5:1.

4.1.2 | Rheology

Figure 2 depicts the values of the complex viscosity of the various FR resin formulations in comparison to two

reference systems: E100 without FRs and E90InSi10 without intumescent. The trends for the viscosity versus temperature curves are in good agreement with DGEBA-DICY-urone formulations reported in the literature.^{37,38} As typically seen, the complex viscosities of the resin formulations are highest starting at room temperature due to a reduction in intermolecular forces and stronger interactions between the epoxy molecules, causing a decreased resistance to flow. Around 140°C , the viscosities of the resins start to increase due to cross-linking and curing reactions leading to solid formation. Here, it is evident that the addition of the various FRs to DGEBA has a minimal effect on the complex viscosity of the resin formulations due to the low loading of 10% of the various FRs. The viscosity is nearly independent of the type of FRs, or morphology used in this case. This behavior indicates that first, the dilution effect due to the fillers is not substantial enough to affect the resin's viscosity. Second, the filler particles evenly distribute themselves in the resin after dispersion, and neither hinder the flow of the resin, nor cause unwanted fluctuations. The lower and higher limits for prepreg processing lie between the complex viscosity values of 10 and 50,000 mPa.s, as depicted

TABLE 5 Summary of curing properties of the various resin formulations.

Sample	Min viscosity (mPa s)	Gel point (°C)	Curing onset (°C)	Peak curing (°C)	Curing enthalpy (J/g)
E100	28 ± 1	147 ± 2	145 ± 0.4	153 ± 0.7	-341 ± 4
E90InSi10	27 ± 1	153 ± 4	149 ± 1	157 ± 1	-317 ± 13
E90InSi2MPP8	29 ± 5	152 ± 4	147 ± 4	157 ± 4.5	-302 ± 53
E90InSi2APP8	23 ± 3	150 ± 3	145 ± 4	154 ± 3	-297 ± 37
E90InSi2SiAPP8	27 ± 5	149 ± 6	144 ± 5	153 ± 5	-279 ± 18

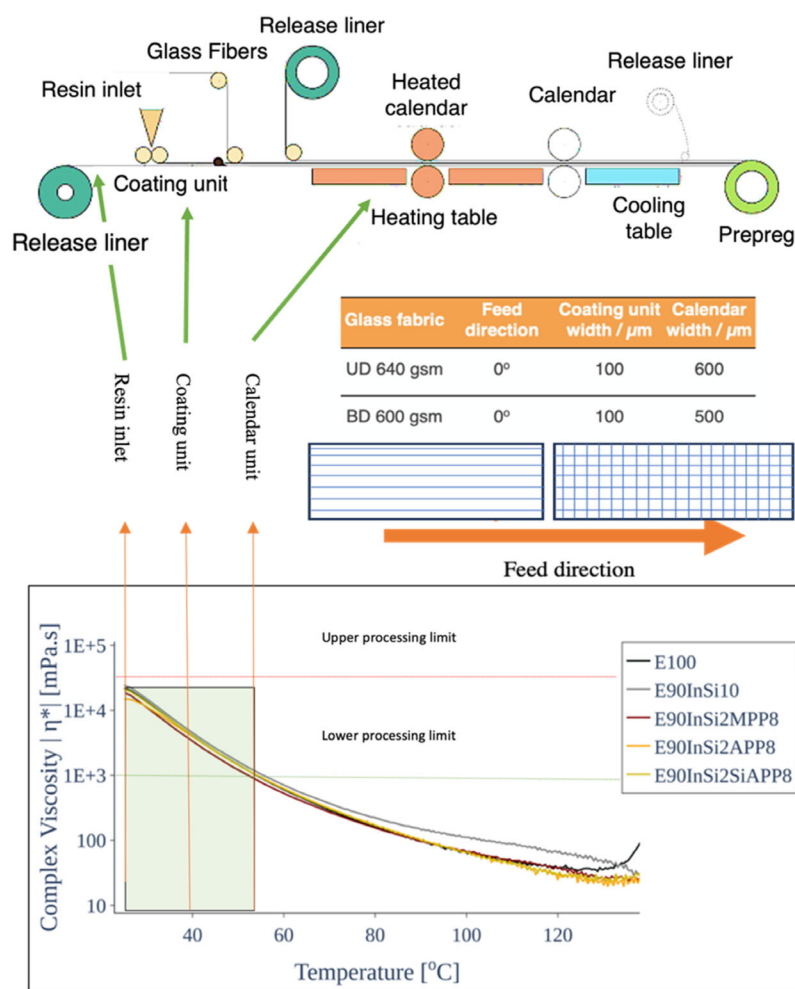


FIGURE 2 Complex viscosity versus temperature curves of various formulations in neat DGEBA and related prepreg line conditions (left). Crossover points of the storage (G') and loss modulus (G'') values to obtain the gel points of the resin formulations (right).

in Figure 2 by the green and red dotted lines parallel to the x -axis. The initial viscosity does not exceed 50,000 mPa.s for any of the formulations, and the lower viscosity limit for these systems lies at a temperature of approximately 50°C.

Thus, the processing temperatures were gradually increased from the resin inlet (25°C) to the coating unit (40°C) followed by the calendar unit (50°C) in the prepreg line. This was chosen to prevent thinning of the

resin before coating and to achieve a homogenous distribution across the fibers during impregnation. Here, the approximate gel points of the various formulations are compared using the crossover points of the storage (G') and loss modulus (G'') values. This is depicted in the temperature range between 140 and 160°C in comparison with the reference systems in Figure 2. The extracted approximate gel point temperatures for the various formulations are also summarized in the same figure and

represent the point where the polymer chains within the resin no longer have the cooperative movements necessary for strain relaxation. It is apparent that the addition of the FRs does not significantly affect the gelation and the subsequent curing properties of DGEBA cured with DICY and urone. The gel points of the FR containing resins E90InSi2MPP8, E90InSi2APP8, and E90InSi2SiAPP8 lie between the gel point values for the reference systems E100 at $147 \pm 2^\circ\text{C}$ and E90InSi10 at $153 \pm 4^\circ\text{C}$. Thus, the replacement of 10% w/w of InSi in the resin with an 8:2 ratio of MPP, APP, and SiAPP to InSi lowers the gel point of the resin system and brings it even closer to the reference value for E100.

4.2 | Fiber volume content and filler dispersion in the composites

The FVC was tested via in-process weighing of the prepregs before and after resin impregnation. Additionally, this was measured using the composites via TGA under synthetic air and the residual volume was calculated.

It was possible to achieve a FVC of 55%–60% during the trials according to the in-process measurements, which are typically targeted for structural reinforcements.³ The TGA data carried out on the cured composites shows that the residual volume ranges from 35% to 65% as shown in Figure 3. This is in-line with typical values for resin content reported in the literature for uncured versus cured prepregs targeted with a FVC of 50%–60% and reducing to 45%–50% after cure.^{15,39} The FVC values are most agreeable (<10% difference between TGA and in-process values) for the resins, with E90InSi2APP8 being the most consistent in both UD and BD composites. However, the FVCs of the prepregs E90InSi2SiAPP8:GF-UD, E90InSi2SiAPP8:GF-BD, and E90InSi2MPP8:GF-BD especially, deviate >10% for the

TGA values compared to the in-process values. For the systems containing SiAPP, indicates potential undesirable covalent interactions between the silane coating of the APP and the standard sizing used in the prepregs, which normally consist of organosilanes and other complex coupling agents.⁴⁰ For the system containing MPP, this signifies the compatible chemical structures of MPP and DGEBA, as shown in Figure 1, which improve the adhesion of the resin to the fibers. This causes a decrease in the FVC, particularly in the BD prepregs with improved resin flow. Thus, despite similar processing parameters, the FVC is more consistently controllable for the UD and BD composites containing E90InSi2APP8.

The distribution of the dispersed FRs in the composites is visualized in Figure 4. The first images show the reference composites E100:GF UD and E100:GF BD containing no FR fillers. It appears that the FRs are distributed in the resin rich regions (in the case of E90InSi2MPP8:GF BD, E90InSi2APP8:GF UD, and E90InSi2APP8:GF BD). In all other cases, the FRs are sparsely dispersed and are not distributed among the resin-rich and poor regions uniformly. Where the fillers are uniformly positioned, they are also found in the resin rich regions, which also penetrate the interior regions despite the high density of the glass fibers at 600 g/m^2 . There are more agglomerates visible in the composites containing APP in comparison to those containing SiAPP. The orientation of the fillers does not show a fixed pattern. When preparing the UD prepregs, it was observed that the resin has a higher tendency to bleed out of the edges of the fiber mats, while no such behavior was observed for the BD prepregs. This is a result of the availability of limited flow pathways across the UD prepregs, which also causes increased filtration of the dispersed fillers. Thus, the BD composites are less likely to filter out the solid fillers in this case. Despite the

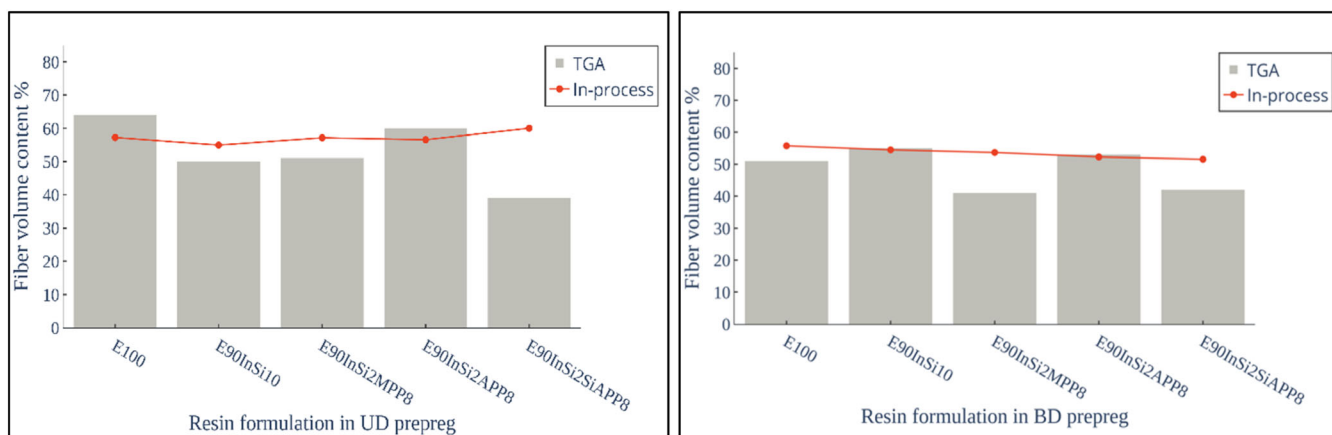


FIGURE 3 Fiber volume content in % in UD and BD GFRECs compared with in-process measurement and TGA under air.

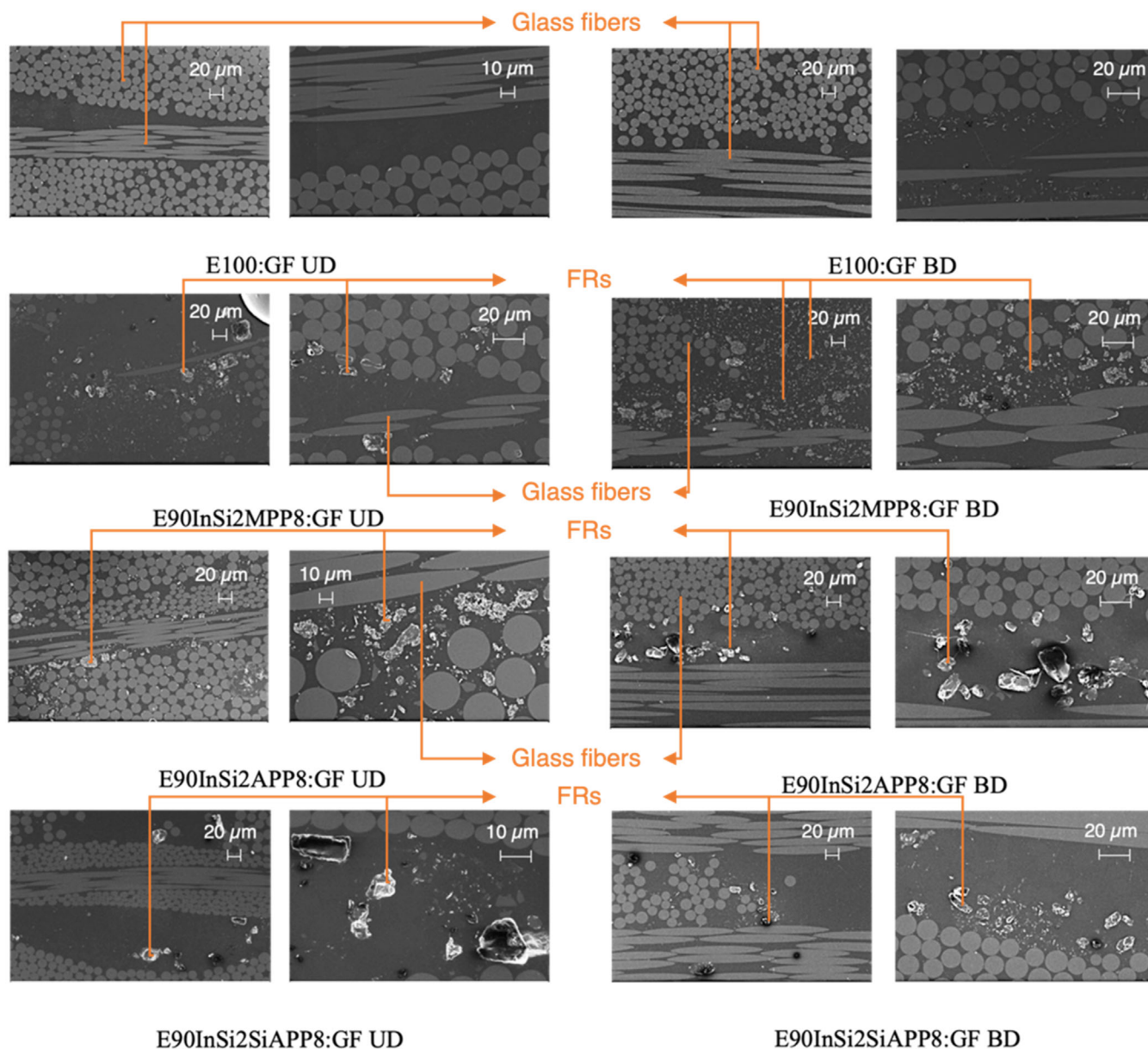


FIGURE 4 SEM images of the various UD (left) and BD (right) composites.

proposed improved processability of SiAPP in epoxy resins in literature,⁴¹ this does not reflect upon transfer to the composites. This phenomenon possibly results from interactions with the commercial sizing on the glass fibers. Consequently, this causes less than ideal filler-matrix-fiber interactions and, thus, increased filtration effects on the SiAPP particles. Considering the optimal processing conditions, only the resin matrix containing APP + InSi is viable for producing UD/BD composites with a FVC of 57%–60% for balancing mechanical performance and potential part quality.⁴² For all the others, further process optimization would be required such as the development of monitoring techniques to observe resin-fiber-matrix interaction and contents in-line.

4.3 | Mechanical behavior of the resins and composites

4.3.1 | Fracture toughness and interlaminar shear strength (ILSS) at room temperature

Figure 5 represents the K_{IC} and G_{IC} values of the resin formulations containing the various phosphate-based flame-retardant formulations. The fracture toughness of the resin formulation DGEBA + DICY + UR400 in the stoichiometric ratio 100:6.51:1 without FRs (E100) at $0.54 \text{ MPa m}^{1/2}$ is close to the value of $\sim 0.61 \text{ MPa m}^{1/2}$ reported in literature.^{43,44} A slight increase in both the K_{IC} and G_{IC} values is apparent when comparing the neat resin

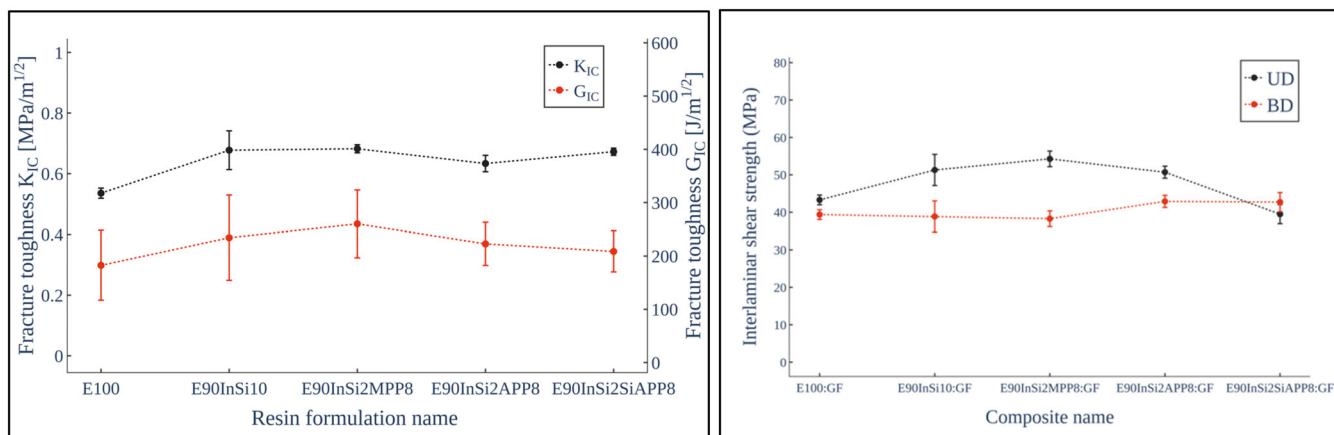


FIGURE 5 K_{IC} and G_{IC} values of the various neat resin formulations (left) and interlaminar shear strength properties of the various UD and BD composites (right).

to E90InSi10/E90InSi2SiAPP8 (+24%), E90InSi2MPP8 (+26%), and E90InSi2APP8 (+16%) potentially due to a reinforcing effect of the fillers at 10% loading in the resin. Some potential mechanisms for this include crack deflection or particle bridging that hinder crack propagation via stress redistribution in the resin matrix.⁴⁵ The intrinsic fracture toughness of the resin matrix can improve the composite's overall ability to resist crack propagation and failure.

This is mirrored in the ILSS data of several of the composites as shown in Figure 5 (right). In the UD composites, the ILSS of the reference sample E100:GF lies at 43 ± 1.3 MPa. For E90InSi10:GF, it increases by 19%, for E90InSi2MPP8:GF by 25%, and for E90InSi2APP8:GF by 17%. However, for E90InSi2SiAPP8:GF, the ILSS decreases by 9%. From the SEM results as well as the rheology results, this is likely not due to resin dilution or particle agglomeration. Since the ILSS value of E90InSi2SiAPP8:GF in the BD composite nearly overlaps with this value and is also higher than for the other formulations in the BD composites, it is apparent that this is not due to the lower FVC of 35% obtained from the TGA data. For all the BD composites, the reference sample E100:GF has an ILSS value of 39.4 ± 0.7 MPa. This decreases by about 12%–13% for E90InSi10:GF and E90InSi2MPP8:GF. For both E90InSi2APP8:GF and E90InSi2SiAPP8:GF, it increases by 9%. The average ILSS values of all the UD composites are about 10%–15% higher than that of the BD composites. In the UD composites, all the glass fibers are arranged parallel to one another, which enables them to effectively withstand the applied load along their length, resulting in a greater ILSS. Conversely, in BD composites, the fiber configuration yields a reduced load-bearing capacity compared to UD composites because half of the fibers are not aligned with the applied load, resulting in a less efficient load transfer.⁴⁶

4.3.2 | Dynamic mechanical analysis (DMA)

Considering that the UD composites are tested in a direction 90° to the orientation of the fibers and the BD composites are tested parallel to the fibers layered along the 90° direction, the storage modulus of E100:GF UD is lower than the latter. The storage moduli of the resin formulations are three times lower than that of the GFRECs. The storage moduli for all the systems decrease slightly with temperatures from 25 to 140°C , after which they sharply decrease and reach 0 at $\sim 160^\circ\text{C}$.

Moreover, the resins containing the FRs at 10% w/w have higher storage moduli than the formulation E100 without FRs due to the potential reinforcing effects of the particulate fillers (also seen in their fracture toughness data in Figure 5), causing reduced chain mobility in the matrix via increased matrix-filler interactions. Consequently, the resins with FRs have $\tan \delta$ values negligibly (around 3%) higher than E100. For both the UD and BD composites, the storage moduli decrease more steeply than the resins with increasing temperature and reach 0 Pa around 150°C . For the UD composites, the presence of the glass fibers as well as the particulate fillers causes potential additional relaxation processes leading to a broadening of the $\tan \delta$ peaks. This broadening is less pronounced in the BD composites, and the $\tan \delta$ peaks are nearly double that of the UD composites, indicating more effective load transfer and energy absorption at the interface between the EP resin and BD fibers, implying good adhesion. The storage moduli of E90InSi10:GF BD and E90InSi2MPP8:GF BD are higher than that of E100:GF BD and nearly overlap, indicating no impact of replacing eight parts of InSi with MPP. Replacing InSi with APP and SiAPP reduces the storage moduli of the UD composites by about 5% across the temperature range of measurement up to 150°C . Figure 6 depicts the glass

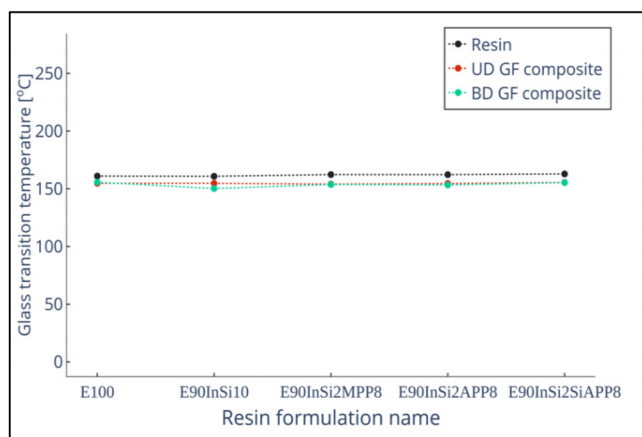


FIGURE 6 Summary of the T_g in the neat resin formulations, UD, and BD composites.

transition temperatures T_g of the resins, UD, and BD composites extracted from the peaks of the $\tan \delta$ values obtained from the DMA data, as shown in Figure 7. The T_g of the resin formulations with or without fillers do not deviate significantly from $\sim 160^\circ\text{C}$. Similarly, for the UD and BD composites, apart from the reference system E90InSi10:GF BD, the T_g lies at $\sim 155^\circ\text{C}$. Hence, the addition of MPP/APP/SiAPP in combination with InSi at 10% w/w in the resin and their transfer to the composites. Thus, at the outset, it would seem as though the use of these different solid flame retardants does not negatively affect the processability, filler-matrix adhesion, or curing behavior of the resins and composites. This contrasts with FR formulations for EP containing reactive species such as DOPO, where Häublein et al.⁴⁷ reported that the T_g of a Novolac EP was found to decrease by almost 40°C with increasing P content up to 3% w/w. Thus, the filler dispersions do not interfere with the cross-linking and curing reactions of the DGEBA formulation.

4.3.3 | Flexural properties at room temperature

Figure 8 shows the flexural modulus (E_F), flexural strength (σ_F) at failure and the corresponding strain at failure (ϵ_F) for the resins, UD, and BD composites.

The flexural modulus of the reference resin E90InSi10 is only 4% higher than that of the reference E100 without FRs. The resin formulations where InSi is replaced by MPP, APP, and Si-APP show an 8%, 7%, and 7% decrease in E_F , respectively. The decrease in ϵ_F for the composites containing FR EP is even more negligible, with a value of $\sim 4\%$ for both UD and BD composites. Thus, the proportion of the fillers in the resin matrix is not significant

enough to cause a degradation in the bending properties of the resins and composites at room temperature, and this does not vary significantly between the variations of polyphosphates used in the resin matrix.

4.4 | Fire behavior and post-fire analysis

4.4.1 | Fire residue thickness and modes of action

The samples' thickness and fire residues were measured before and after the samples were tested in the cone calorimeter. The results are shown in Figure 9, where the thickness of the residues on the glass fiber reinforced composite containing MPP/APP/SiAPP: InSi EP formulations is only 15%–20% of that of the epoxy resin samples due to the modes of action of the FRs in the gas/condensed phases in the resin being partially or entirely suppressed when transferred to the glass fibers reinforced composites. The modes of action will be investigated in detail in a future publication.

All the tested samples had a thickness of 4.0 ± 0.3 mm before being exposed to the fire. For the epoxy resin after the fire, the residue had a thickness of 10 mm. The sample with InSi increased the residue by ~ 20 mm after the fire. The residue of the MPP/APP/SiAPP samples increased by ~ 44 , 53, and 59 mm, respectively, when compared to the epoxy resin without any FRs. In comparison with the resins, the composite sample with epoxy resin and unidirectional glass fiber had only a 3 mm residue increase, and the UD composite samples with the addition of flame retardants (MPP, APP, and SiAPP) had an increase of 3, 6, and 7.3 mm in the residue respectively. The sample with epoxy resin and BD GFs had just an increase of 3.5 mm in the residue thickness. The BD composites containing flame retardants (MPP, APP, and SiAPP) increased by 3.5, 2, and 4.7 mm, respectively. The fire residues in the sample with epoxy resin, InSi, and glass fibers (UD and BD) increased by 3.7 and 3.5 mm, respectively, compared to the sample's original thickness (4.0 mm) before the fire.

The modes of action are quantified with the equations shown in previous studies.^{48,49} The sample with 8% MPP + 2% InSi + UD GFs had a char reduction up to 29% of char in the condensed phase compared to the sample with 8% MPP and 2% InSi, while in the gas phase (fuel dilution and flame inhibition) it increased to 9%. The sample with 8% MPP + 2% InSi + BD GFs increased by 5% in the gas phase (fuel dilution and flame inhibition) and charring in the condensed phase

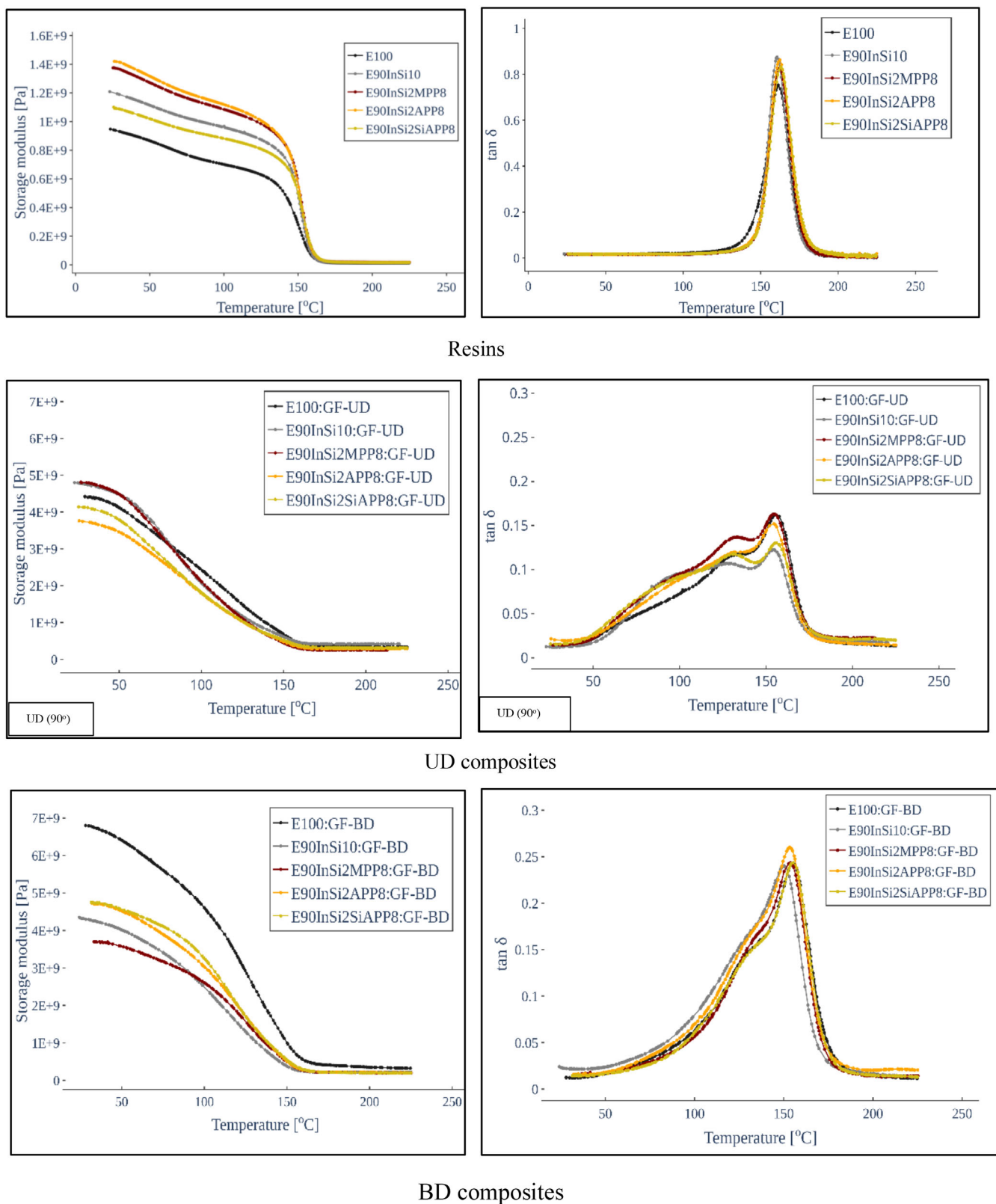


FIGURE 7 DMA curves of the three FR formulations in comparison to the reference systems in the BD composites. Note that the scale of the $\tan \delta$ graph for the resins is three times that of the composites.

was reduced by 5%. The sample with 8% APP + 2% InSi + UD GFs had complete suppression of the charring in the condensed and gas phases (fuel dilution and

flame inhibition). The sample with 8% APP + 2% InSi + BD GFs increased only 1.9% in the gas phase (fuel dilution and flame inhibition) and charring in the

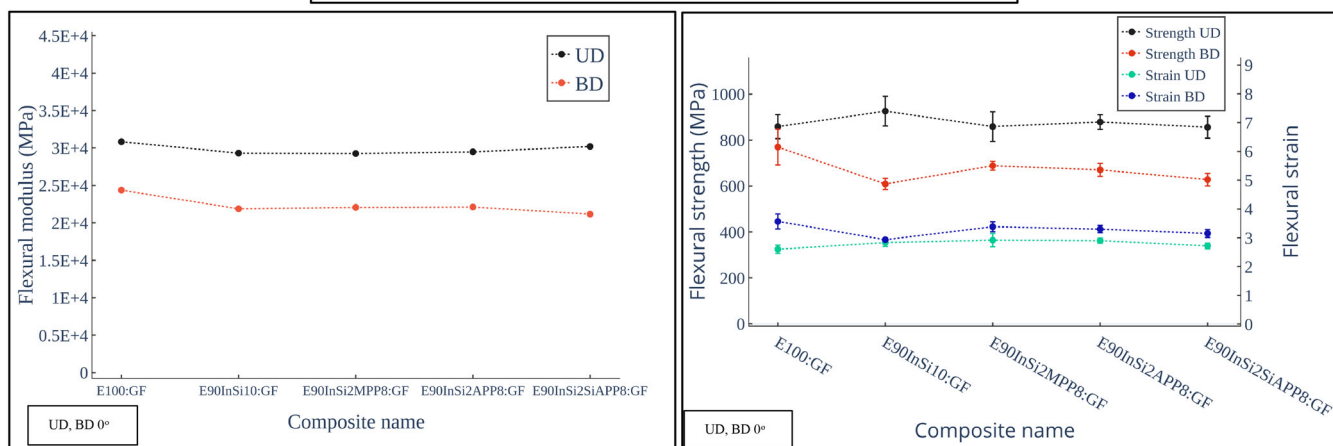
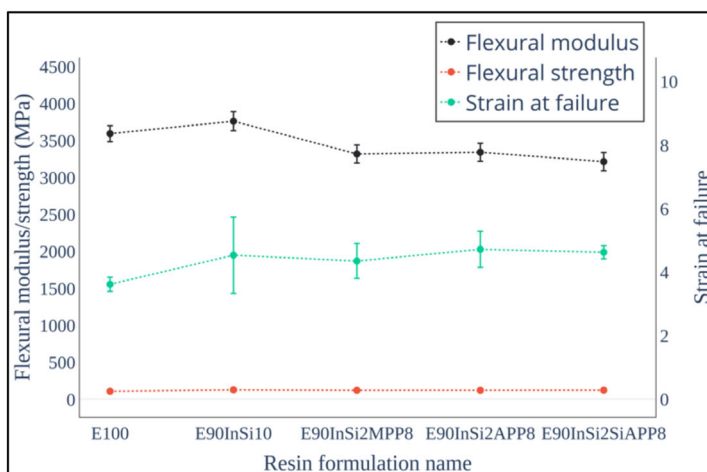


FIGURE 8 Flexural properties of the neat resins (top) and composites (bottom left and bottom right).

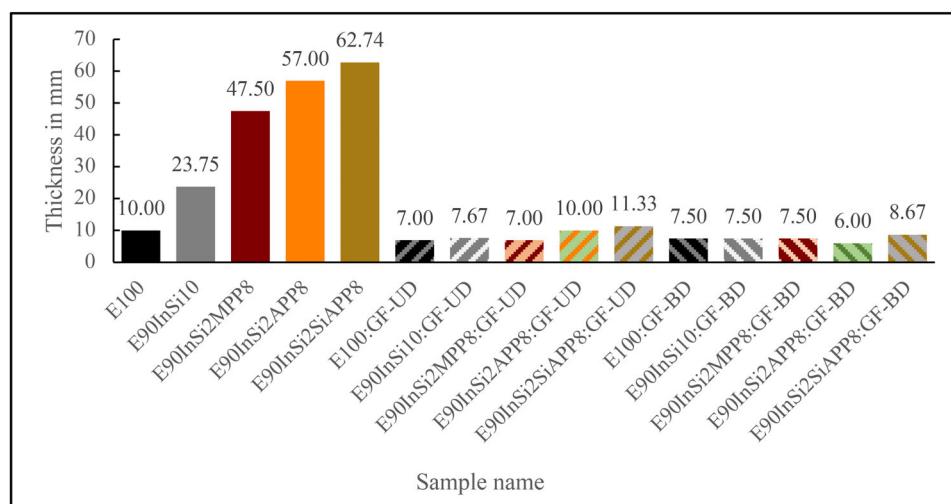


FIGURE 9 Fire residue thickness of epoxy resins and composites with UD and BD GFs.

condensed phase was suppressed. The gas phase activity (fuel dilution and flame inhibition) in the samples with 8% SiAPP + 2% InSi + UD and BD GFs increased by 4% and 3%. It decreased by 12% with UD-GF and 24% with BD-GF in the char in the condensed phase.

All these results suggest that with the addition of FRs, there is a higher increase in the thickness of the fire residue and a reduction of the fire load compared to epoxy resin. An increase in all the modes of action in the condensed and gas phase (charring, protective layer, flame

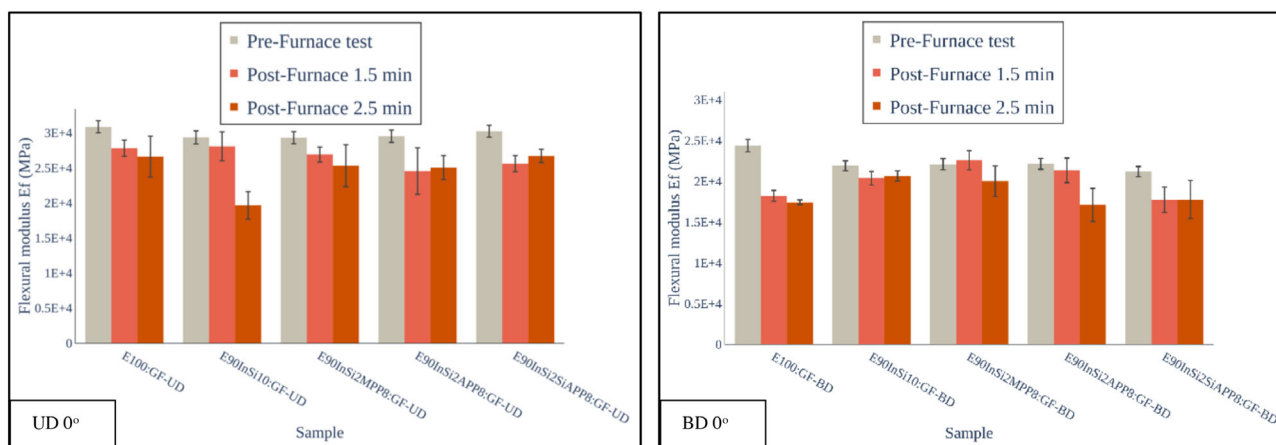


FIGURE 10 Flexural properties of the GF composites after exposure in a furnace oven at 400°C.

inhibition, and fuel dilution) is observed for all three FRs (APP, MPP, and SiAPP).

With the addition of GFs, there is a slight decrease in the thickness of the fire residue, a higher reduction of the fire load in comparison to the samples with only FRs, an increase of the protective layer in the condensed phase, and a suppression of the charring in the condensed phase. It is also essential to consider that the average weight of the GFs in the samples with UD GFs was around 71 wt%, and with BD GFs, it was 68 wt% and that means that the fiber weight percentage is much higher than the resin weight; therefore, the impact of the glass fibers on the fire behavior of the resins with and without flame retardants and the fire residue is relevant. This result can also be related to the change in melt flow and the wicking effect that the glass fibers are causing under fire. This hypothesis will be investigated and verified in a future study.

4.4.2 | Post-furnace flexural properties

Exposing BD and UD EP GF composites within a furnace at 400°C for 1.5 and 2.5 min in general, causes significant reductions to their flexural moduli after 2.5 min of exposure as shown in Figure 10. These changes are primarily attributed to the degradation of matrix-fiber adhesion.¹⁶

Since 400°C is well above the T_g of the DGEBA-DICY-urone resin system (~160°C), the matrix softens, leading to a reduction in stiffness. Additionally, extended exposure to high temperatures can cause some degradation in the interface between the resin matrix and the glass fibers, further affecting the composite's mechanical properties. After an exposure time of 3 min, the laminates were completely delaminated, and mechanical testing was unviable. On

average, the % reduction in E_F for the UD GFs is comparable to that of the BD GFs after 1.5 min (10%–11%) and 2.5 min (16%–17%). The decrease in E_F after 1.5 min furnace exposure is highest for E90InSi2APP8:GF-UD, E90InSi2SiAPP8:GF-UD at 17% and 15%. However, in the case of the BD fibers, the decrease is highest for E100:GF-BD, which does not contain any FRs, at 25%, while the E_F of E90InSi2SiAPP8:GF-UD was second at 16%. The decrease in E_F after 2.5 min furnace exposure is highest for E90InSi10:GF-UD at 33% and second, for E90InSi2APP8:GF-UD at 15%. In the case of the BD fibers, the decrease is highest for E100:GF-BD, which does not contain any FRs, at 28%, followed by E90InSi2APP8:GF-UD at 23%. In some cases, even a slight increase in the E_F observed after furnace exposure, and increased degradation effects on the edges of the samples are unavoidable. In future work, it would thus be necessary to conduct post-fire mechanical analysis with the ignition of the samples, using a more reproducible method, with controlled heat fluxes.

5 | CONCLUSION

In this study, a combination of melamine polyphosphate (MPP), ammonium polyphosphate (APP), and silane-coated ammonium polyphosphate (SiAPP) flame retardants (FRs) with low-melting inorganic silicates (InSi) were loaded at 10% by weight, in an 8:2 ratio of intumescent to InSi within a diglycidyl ether of bisphenol A (DGEBA) epoxy resin cured with a dicyandiamide hardener (DICY) and a urone accelerator. These formulations were compared with a system containing only 10% w/w of InSi and were all successfully transferred to unidirectional (UD) and bidirectional (BD) glass fiber composites via prepreps for processing, pre-fire mechanics, and post-

furnace mechanical analysis. Advantageously, the addition of the FRs did not significantly impact the glass transition temperature or the processing properties of the DGEBA resin. However, it was found that the fire residues obtained from cone calorimetry for composites containing FRs were only 15–20% of the thickness of those from the resins. There was also a suppression of the FR mode of action upon transfer of the FRs to the composites which contrasts with what was observed in the resin. Currently, the resin matrix containing APP + InSi was most viable for transfer to UD/BD composites with a controllable fiber volume content of 57%–60%. The study reveals an enhancement in both the K_{IC} and G_{IC} values when comparing the neat resin to E90InSi10/E90InSi2-SiAPP8 (+24%), E90InSi2MPP8 (+26%), and E90InSi2APP8 (+16%) potentially due to a toughening effect of the fillers at 10% w/w loading in the resin. The average interlaminar shear strength (ILSS) values of all the UD composites surpassed that of the BD composites by 10%–15%.

The assessment of post-furnace flexural properties in composites is used here as a pivotal first step to understand the challenges surrounding post-fire mechanical studies. Notably, at room temperature, the decrease in ϵ_F for the composites containing FR EP is negligible, with a decrease of ~4% on average for both UD and BD composites. However, when subjecting the composites to a furnace at 400°C, a significant reduction in flexural moduli was observed after 2.5 min of exposure, and after 3 min, complete delamination occurred. This reveals a critical challenge in obtaining viable samples to test the post-fire flexural mechanics of the composites after burning, even under short exposure times. In a future study, a suitable method for testing the post-fire flexural properties of the composites under ignition will be developed. The differences in processing resulting from moderately and highly filled FR systems will thus be investigated to improve the fire residues and recover the modes of action of the FRs in the composites.

ACKNOWLEDGMENTS

The authors would like to thank the German Research Foundation (DFG) with the grant number AL 474/53-1 and DFG SCHA730/26-1 for funding the project and Prof. Dr.-Ing. Volker Altstädt for his contribution to the project. The authors thank Keylab of the Bavarian Polymer Institute and Annika Pfaffenberger for their contribution to the SEM measurements. The authors would like to thank Christian Bauer and Alexandra Krasnik for assistance with sample preparation, and Ute Kuhn and Andreas Mainz for assistance with sample testing. Open Access funding enabled and organized by Projekt DEAL.

DATA AVAILABILITY STATEMENT

The data is available from the authors upon reasonable request.

ORCID

Bernhard Schartel  <https://orcid.org/0000-0001-5726-9754>

Holger Ruckdäschel  <https://orcid.org/0000-0001-5985-2628>

REFERENCES

1. Epoxy Europe. *Epoxy Resins Updated Socio-Economic Assessment*; 2019. Accessed April 6, 2023. <https://epoxy-europe.eu/epoxies/european-industry-socio-economic/>
2. Maxineasa SG, Taranu N. 24–Life cycle analysis of strengthening concrete beams with FRP. *Eco-Efficient Repair and Rehabilitation of Concrete Infrastructures. Woodhead Publishing Series in Civil and Structural Engineering*. Woodhead Publishing; 2018:673–721. doi:10.1016/B978-0-08-102181-1.00024-1
3. Zweben CH. Composites: overview. In: Bassani F, Liedl GL, Wyder P, eds. *Encyclopedia of Condensed Matter Physics*. Elsevier; 2005:192–208. doi:10.1016/B0-12-369401-9/00545-3
4. Häublein M, Demleitner M, Altstädt V. Fire behavior and flame-retardant properties of application-oriented fiber-reinforced polymers (FRPs). *Compos Materials*. Elsevier; 2021; 383–417. doi:10.1016/B978-0-12-820512-9.00008-3
5. Romero-Zúñiga GY, Navarro-Rodríguez D, Treviño-Martínez ME. Enhanced mechanical performance of a DGEBA epoxy resin-based shape memory polymer by introducing graphene oxide via covalent linking. *J Appl Polym Sci*. 2022; 139(2):51467. doi:10.1002/app.51467
6. Huo S, Song P, Yu B, et al. Phosphorus-containing flame retardant epoxy thermosets: recent advances and future perspectives. *Prog Polym Sci*. 2021;114:101366. doi:10.1016/j.progpolymsci.2021.101366
7. Zhang W, Li X, Fan H, Yang R. Study on mechanism of phosphorus–silicon synergistic flame retardancy on epoxy resins. *Polym Degrad Stab*. 2012;97(11):2241–2248.
8. Döring M, Ciesielski M, Heinzmann C. Synergistic flame retardant mixtures in epoxy resins. *Fire and Polymers VI: New Advances in Flame Retardant Chemistry and Science*. Vol 1118. ACS Symposium Series. American Chemical Society; 2012:295–309. doi:10.1021/bk-2012-1118.ch020
9. Fang M, Qian J, Wang X, Chen Z, Guo R, Shi Y. Synthesis of a novel flame retardant containing phosphorus, nitrogen, and silicon and its application in epoxy resin. *ACS Omega*. 2021;6(10): 7094–7105. doi:10.1021/acsomega.1c00076
10. Schartel B, Balabanovich AI, Braun U, et al. Pyrolysis of epoxy resins and fire behavior of epoxy resin composites flame-retarded with 9,10-dihydro-9-oxa-10-phosphaphenanthrene-10-oxide additives. *J Appl Polym Sci*. 2007;104(4):2260–2269. doi:10.1002/app.25660
11. Perret B, Schartel B, Stöß K, et al. A new halogen-free flame retardant based on 9,10-dihydro-9-oxa-10-phosphaphenanthrene-10-oxide for epoxy resins and their carbon fiber composites for the automotive and aviation industries. *Macromol Mater Eng*. 2011;296(1):14–30. doi:10.1002/mame.201000242

12. Bifulco A, Varganici C, Rosu L, Mustata F, Rosu D, Gaan S. Recent advances in flame retardant epoxy systems containing non-reactive DOPO based phosphorus additives. *Polym Degrad Stab.* 2022;200:109962. doi:10.1016/j.polyimdegradstab.2022.109962
13. Rajaei M, Kim NK, Bickerton S, Bhattacharyya D. A comparative study on effects of natural and synthesised nano-clays on the fire and mechanical properties of epoxy composites. *Compos B Eng.* 2019;165:65-74. doi:10.1016/j.compositesb.2018.11.089
14. Neumeyer T, Bauernfeind A, Eigner V, Mueller C, Pramberger K, Altstaedt V. Novel epoxy prepreg resins for aircraft interiors based on combinations of halogen-free flame retardants. *CEAS Aeronaut J.* 2018;9(1):235-248.
15. Pawelski-Hoell C, Bhagwat S, Altstädt V. Thermal, fire, and mechanical properties of solvent-free processed BN/boehmite-filled prepreps. *Polym Eng Sci.* 2019;59(9):1840-1852.
16. Mouritz AP, Gibson AG. *Fire Properties of Polymer Composite Materials.* Springer Science & Business Media; 2007.
17. Lim WP, Mariatti M, Chow WS, Mar KT. Effect of intumescent ammonium polyphosphate (APP) and melamine cyanurate (MC) on the properties of epoxy/glass fiber composites. *Compos B Eng.* 2012;43(2):124-128.
18. Wang X, Hu Y, Song L, et al. Effect of a triazine ring-containing charring agent on fire retardancy and thermal degradation of intumescent flame retardant epoxy resins. *Polym Adv Technol.* 2011;22(12):2480-2487. doi:10.1002/pat.1788
19. Liu L, Zhang Y, Li L, Wang Z. Microencapsulated ammonium polyphosphate with epoxy resin shell: preparation, characterization, and application in EP system. *Polym Adv Technol.* 2011; 22(12):2403-2408. doi:10.1002/pat.1776
20. Ares Elejoste P, Allue A, Ballester J, Neira S, Gómez-Alonso JL, Gondra K. Development and characterisation of sustainable prepreps with improved fire behaviour based on furan resin and basalt fibre reinforcement. *Polymers.* 2022; 14(9):1864. doi:10.3390/polym14091864
21. Zhang X, Zhang F, Zhang W, Tang X, Fan HJS. Enhance the interaction between ammonium polyphosphate and epoxy resin matrix through hydrophobic modification with cationic latex. *Colloids Surf A Physicochem Eng Asp.* 2021;610:125917. doi:10.1016/j.colsurfa.2020.125917
22. Ricciardi MR, Antonucci V, Zarrelli M, Giordano M. Fire behavior and smoke emission of phosphate-based inorganic fire-retarded polyester resin. *Fire Mater.* 2012;36(3):203-215.
23. Schmidt C, Ciesielski M, Greiner L, Döring M. Novel organophosphorus flame retardants and their synergistic application in novolac epoxy resin. *Polym Degrad Stab.* 2018;158:190-201. doi:10.1016/j.polyimdegradstab.2018.09.001
24. Ratna D. *Handbook of Thermoset Resins.* ISmithers Shawbury; 2009.
25. Wu GM, Schartel B, Kleemeier M, Hartwig A. Flammability of layered silicate epoxy nanocomposites combined with low-melting inorganic ceepree glass. *Polym Eng Sci.* 2012;52(3):507-517. doi:10.1002/pen.22111
26. Liu W, Pan YT, Zhang J, et al. Low-melting phosphate glasses as flame-retardant synergists to epoxy: barrier effects vs flame retardancy. *Polym Degrad Stab.* 2021;185:109495.
27. Sut A, Greiser S, Jäger C, Schartel B. Synergy in flame-retarded epoxy resin. *J Therm Anal Calorim.* 2017;128(1):141-153. doi:10.1007/s10973-016-5934-4
28. Synergy in flame-retarded epoxy resin | SpringerLink. Accessed April 6, 2023. doi:10.1007/s10973-016-5934-4
29. Mouritz AP. Post-fire flexural properties of fibre-reinforced polyester, epoxy and phenolic composites. *J Mater Sci.* 2002; 37(7):1377-1386. doi:10.1023/A:1014520628915
30. Gardiner CP, Mathys Z, Mouritz AP. Post-fire structural properties of burnt GRP plates. *Mar Struct.* 2004;17(1):53-73.
31. Katsoulis C, Kandola BK, Myler P, Kandare E. Post-fire flexural performance of epoxy-nanocomposite matrix glass fibre composites containing conventional flame retardants. *Compos Part A Appl Sci Manuf.* 2012;43(8):1389-1399. doi:10.1016/j.compositesa.2012.03.009
32. Müller B, Poth U. *Coatings Formulation: An International Textbook.* Vincentz; 2006.
33. Demleitner M. *Prepreg Technology at Polymer Engineering.* https://www.polymer-engineering.de/wp-content/uploads/2020/12/Prepreps_at_Polymer_Engineering.pdf
34. Schartel B, Bartholmai M, Knoll U. Some comments on the use of cone calorimeter data. *Polym Degrad Stab.* 2005;88(3):540-547.
35. Hayaty M, Honarkar H, Beheshty MH. Curing behavior of dicyandiamide/epoxy resin system using different accelerators. *Iran Polym J.* 2013;22:591-598.
36. Pascault JP, Williams RJJ. *Epoxy Polymers: New Materials and Innovations.* John Wiley & Sons; 2009.
37. Wu F, Zhou X, Yu X. Reaction mechanism, cure behavior and properties of a multifunctional epoxy resin, TGDDM, with latent curing agent dicyandiamide. *RSC Adv.* 2018;8(15):8248-8258.
38. Gilbert M. *Mechanism and Kinetics of the Dicyandiamide Cure of Epoxy Resins;* 1988. Accessed August 3, 2023. <https://www.semanticscholar.org/paper/Mechanism-and-kinetics-of-the-dicyandiamide-cure-of-Gilbert/44a36df14294cc000db64e06503b9e4ccecfeff5>
39. Halpin JC, Kardos JL, Dudukovic MP. Processing science: an approach for prepreg composite systems. *Pure Appl Chem.* 1983;55(5):893-906. doi:10.1351/pac198355050893
40. Thomason JL. Glass fibre sizing: a review. *Compos Part A Appl Sci Manuf.* 2019;127:105619. doi:10.1016/j.compositesa.2019.105619
41. Wang F, Liao J, Long M, Yan L, Cai M. Facile synthesis of reduced-graphene-oxide-modified ammonium polyphosphate to enhance the flame retardancy, smoke release suppression, and mechanical properties of epoxy resin. *Polymers.* 2023;15(5):1304. doi:10.3390/polym15051304
42. Campbell FC. Chapter 6—Curing: it's a matter of time (t), temperature (T) and pressure (P). In: Campbell FC, ed. *Manufacturing Processes for Advanced Composites.* Elsevier Science; 2004:175-221. doi:10.1016/B978-185617415-2/50007-1
43. Pham TD, Vu CM, Choi HJ. Enhanced fracture toughness and mechanical properties of epoxy resin with rice husk-based nano-silica. *Polym Sci A.* 2017;59:437-444.
44. Kumar S, Krishnan S, Samal SK, Mohanty S, Nayak SK. Toughening of petroleum based (DGEBA) epoxy resins with various renewable resources based flexible chains for high performance

- applications: a review. *Ind Eng Chem Res.* 2018;57(8):2711-2726.
45. Andreasen JH, Karihaloo BL. *Mechanics of Transformation Toughening and Related Topics.* Elsevier; 1996.
 46. Rowe J. *Advanced Materials in Automotive Engineering.* Elsevier; 2012.
 47. Häublein M, Peter K, Bakis G, Mäkimieni R, Altstädt V, Möller M. Investigation on the flame retardant properties and fracture toughness of DOPO and nano-SiO₂ modified epoxy novolac resin and evaluation of its combinational effects. *Materials.* 2019;12(9):1528.
 48. Brehme S, Schartel B, Goebbels J, et al. Phosphorus polyester versus aluminium phosphinate in poly (butylene terephthalate) (PBT): flame retardancy performance and mechanisms. *Polym Degrad Stab.* 2011;96(5):875-884.
 49. Rabe S, Chuenban Y, Schartel B. Exploring the modes of action of phosphorus-based flame retardants in polymeric systems. *Materials.* 2017;10(5):455. doi:10.3390/ma10050455

SUPPORTING INFORMATION

Additional supporting information can be found online in the Supporting Information section at the end of this article.

How to cite this article: Sunder S, Jauregui Rozo M, Inasu S, Schartel B, Ruckdäschel H. A systematic investigation of the transfer of polyphosphate/inorganic silicate flame retardants from epoxy resins to layered glass fiber-reinforced composites and their post-furnace flexural properties. *Polym Compos.* 2024;45(10):9389-9406. doi:10.1002/pc.28416

Supplementary information

1.1 Frequency sweep rheology at initial curing temperature - 100 °C

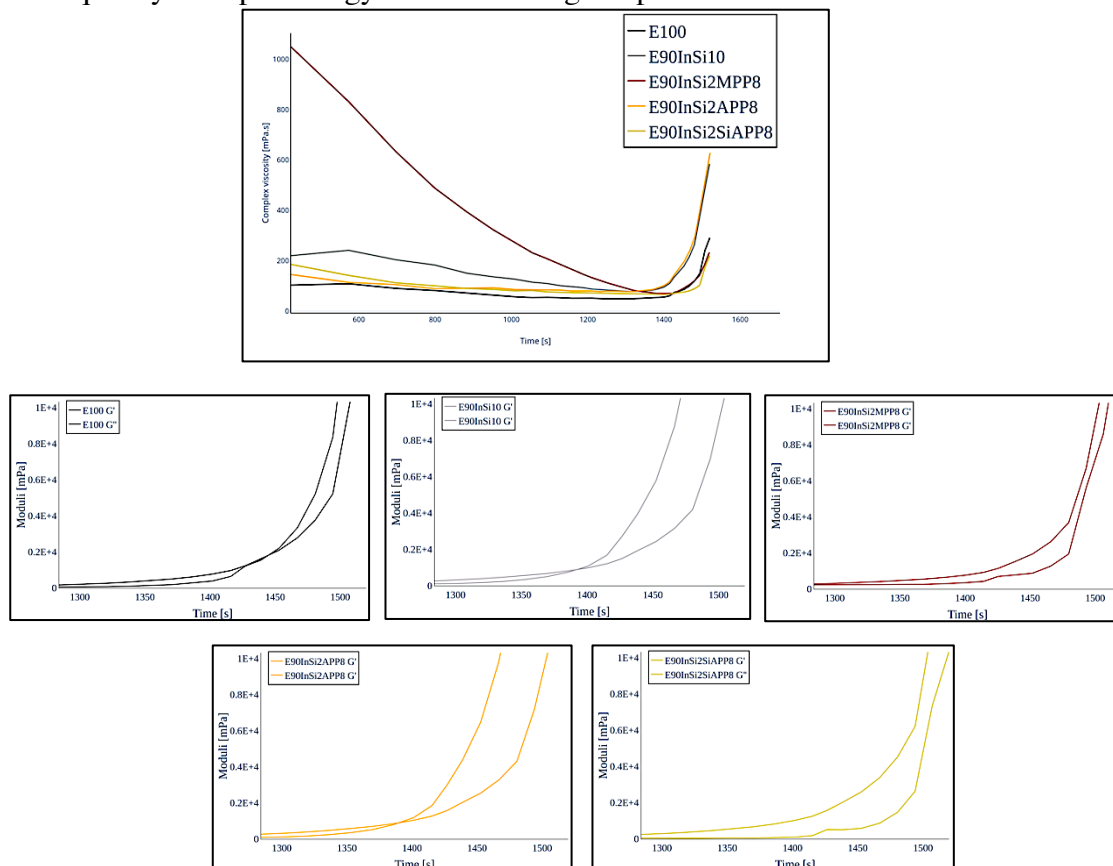


Figure A. Complex viscosity and storage and loss moduli of resin formulations containing various additives at 100 °C

1.2 Particle morphology, size distribution and dispersion in the resin

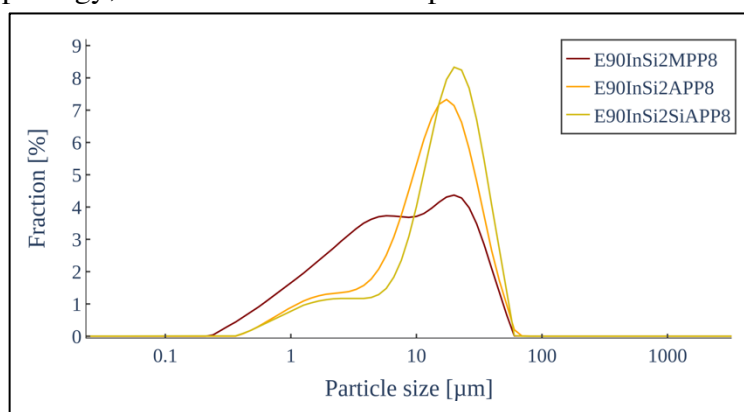


Figure B. DLS analysis of the additive mixtures used for the FR resin formulations

Table 1. Summary of DLS data for additive mixtures used as FRs

Mixture	d_{50} (μm)	d_{90} (μm)
MPP: InSi (8:2)	7	27
APP: InSi (8:2)	13	30
SiAPP: InSi (8:2)	16	33

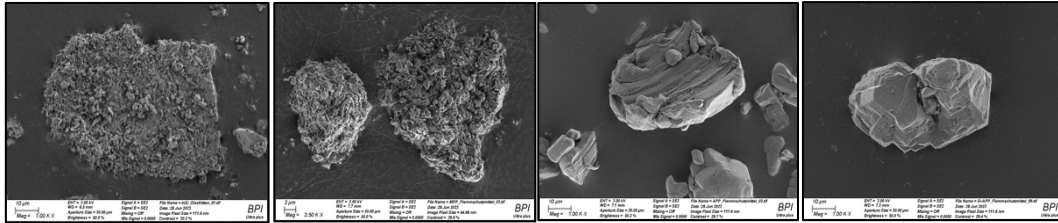


Figure C. SEM images of the particles of InSi, MPP, APP and Si-APP

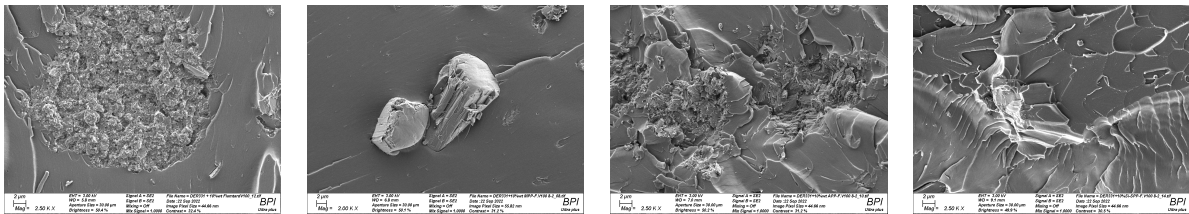


Figure C. SEM images of the surface morphology of the FR resin formulations

1.3 FTIR spectra

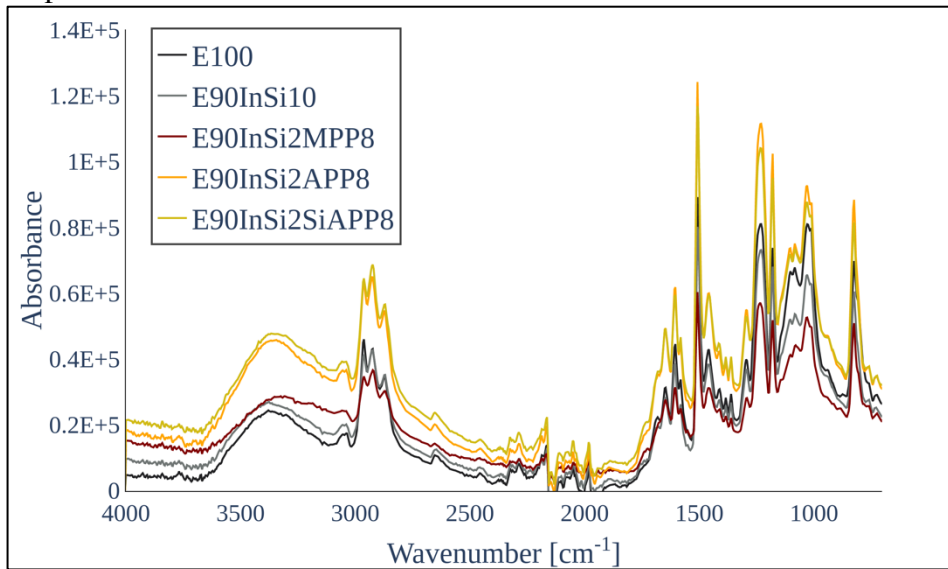


Figure D. FTIR spectra of the various FR resin formulations indicating a lack of structural chemical modifications after incorporation of the FRs